Article citation info:
SHUAI L, ZHENCAI Z, HAO L, GANG S. A system reliability-based design optimization for the scraper chain of scraper conveyors with dependent failure modes. Eksploatacja i Niezawodnosc – Maintenance and Reliability 2019; 21 (3): 392–402, http://dx.doi.org/10.17531/ein.2019.3.5.

Li SHUAI
Zhu ZHENCAI
Lu HAO
Shen GANG

A SYSTEM RELIABILITY-BASED DESIGN OPTIMIZATION FOR THE SCRAPER CHAIN OF SCRAPER CONVEYORS WITH DEPENDENT FAILURE MODES

OPARTA NA NIEZAWODNOŚCI SYSTEMU OPTYMALIZACJA KONSTRUKCJI ŁAŃCUCHA PRZENOŚNIKOWEGO ZGRZEBŁOWEGO O ZALEŻNYCH PRZYCZYNACH USZKODZEŃ

With the incomplete probability information, the joint probability distribution modelling and system reliability-based optimization design of structural systems with failure interactions are challenging problems in the domain of reliability. This article is designed to propose a system reliability-based optimization design method for optimizing the scraper chain with multiple failure modes. Firstly, the common failure modes of the scraper chain are analysed. For each failure mode, a reliability model for the failure of scraper chains is obtained. Secondly, aiming at the joint failure probability modelling problem, a method for estimating the failure probability of the scraper chain based on system reliability is proposed. The reliability of scraper chains is calculated by the stochastic perturbation technique and the four-moment method. And then, the optimization design problem is discussed based on system reliability. And the optimal model is established. Finally, the effectiveness of the method is verified by the illustrative example of scraper chains. The proposed joint failure probability estimation method and design optimization are shown in the example. The results obtained can provide a reference for the optimal design of the scraper chain.

Keywords: *probabilistic analysis; system reliability; Copula; scraper chain; optimization.*

Ze względu na niekompletność danych dotyczących prawdopodobieństwa, modelowanie wspólnego rozkładu prawdopodobieństwa oraz oparte na niezawodności systemu projektowanie optymalizacyjne systemów konstrukcyjnych, w których zachodzą zależności między uszkodzeniami stanowią trudne problemy niezawodnościowe. W artykule zaproponowano metodę optymalizacji konstrukcji łańcucha zgrzebłowego, w której wykorzystuje się obliczenia niezawodności systemu. Ponieważ dla łańcucha tego typu istnieje wiele potencjalnych przyczyn uszkodzeń, w pierwszej kolejności analizowano powszechnie występujące przyczyny uszkodzeń. Dla każdego rodzaju uszkodzenia łańcucha otrzymano model niezawodnościowy. Następnie, mając na uwadze problem modelowania wspólnego rozkładu prawdopodobieństwa uszkodzeń, zaproponowano metodę szacowania prawdopodobieństwa uszkodzenia łańcucha na podstawie niezawodności systemu. Niezawodność łańcuchów zgrzebłowych obliczano za pomocą techniki zaburzeń stochastycznych oraz metody momentu czwartego rzędu. Na podstawie otrzymanej niezawodności systemu, omówiono problem optymalizacji konstrukcji łańcucha oraz wyznaczono model optymalny. Skuteczność proponowanych metod estymacji wspólnego prawdopodobieństwa uszkodzenia i optymalizacji konstrukcji weryfikowano na podstawie przykładu łańcucha zgrzebłowego. Uzyskane wyniki mogą stanowić punkt odniesienia dla optymalnego projektowania łańcuchów zgrzebłowych.

Słowa kluczowe: *analiza probabilistyczna; niezawodność systemu; funkcja kopuły; łańcuch przenośnikowy zgrzebłowy; optymalizacja.*

1. Introduction

In the current coal mining face, the scraper conveyor (Fig. 1) as one of the key equipments for large-scale, high-efficiency and continuous coal mining equipment not only bears the role of coal transportation, but also the running track of the shearer and the shifting point of the hydraulic support [24]. Therefore, the scraper conveyor is throughout the fully mechanized mining face and occupies an extremely important position. As shown in Fig. 1, the scraper conveyor consists of one control cabinet, one double-chain drive system, two double-drive sprockets, one to three drive units and lots of middle troughs. With the development of high-yield and high-efficiency coal mining face, it is urgent to develop large-capacity, long-distance, high-power, high-reliability scraper conveyors [9]. The intent of the reliability-based optimal design is less maintenance or maintenance-free, resulting in objective economic benefits. The scraper chain (Fig. 2) is the core component of the scraper conveyor; its quality and performance directly affect the working efficiency of scraper conveyors. Due to the complexity and the harshness of the working condition, the scraper chain is prone to serious accidents. The coal production performance can be specifically attributed to the reliability of scraper chains. Therefore, it is considered necessary to introduce the structural reliability models throughout the design process to provide a more accurate reliability assessment and parameter optimization for the scraper chain with multiple failure modes.

Random variables such as tensile force, structural dimensions and material properties of the scraper chain may affect its reliability. What's more, in order to meet reliability requirements of the scraper chain, the random variables that have a significant impact on device

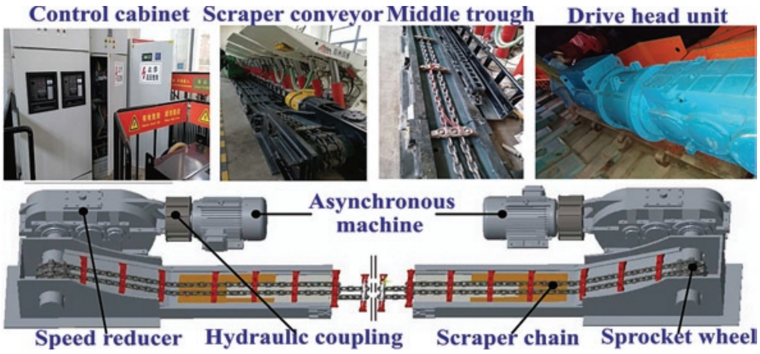

Fig.1 The structure of scraper conveyors

reliability must be constrained [13, 10, 20]. And here, the random distributions are used to deal with the uncertainty, and the exact intervals are replaced by the change intervals of some key parameters in the distribution functions [7]. Then, the most suitable Copula function is selected by the Akaike information criterion (AIC) [1, 11].

As well known, the Pearson correlation coefficient is the most widely used method to describe the correlation between failures, but it is only an approximation of the actual situation, which has great limitations, and cannot reflect the dependency structure between the failures of the scraper chain accurately [14]. And then, the joint probability distribution of multivariate data is constructed to assess the correlation between the diffident failure modes of the scraper chain based on the Copula theory. The Copula function is actually a function that links the joint distribution functions with their respective marginal distribution functions and can be used to describe the correlation between variables. Copulas are favored for two main reasons: the first is that it is a method for studying the dependent measurements; and the second is that the Copula as the starting point for constructing a two-dimensional distribution family can be used for multivariate model distribution and random simulation. The Copula function, as a tool of the interdependence mechanism between variables, contains almost all the dependent information of random variables [22]. If it is impossible to determine whether the traditional linear correlation coefficient can correctly measure the correlation between variables or not, the Copula function is helpful for the analysis of the correlation between variables, and its appearance makes the dependence between variables more perfect. Furthermore, there are many Copula families, which differ in the detail of the dependence they represent such as the Gaussian, Gumbel, Frank, and Clayton Copulas, and so on [19]. And so far, the Copula methods have been proved to be the most effective mathematical tool and can greatly reduce the difficulty of the joint probabilistic modelling [17, 3, 23].

In order to ensure the reliability of the scraper chain, a reliability-based optimization design method is proposed. The system failure probability and the optimization design of the scraper chain are analyzed with the influence of uncertain parameters [2, 15]. The remainder of this paper is structured as follows: In Section 2, the performance functions of the scraper chain are established based on failures of the elongation, contact strength and the tensile strength. In Section 3, the marginal probability of failure is estimated by stochastic perturbation technique and the system failure probability is estimated by the Copulas and narrow bounds. In Section 4, the optimal design based on reliability of the scraper chain with multiple failure modes is described by the mathematical model. In Section 5, the application of the proposed method is illustrated by the probabilistic analysis and optimization design based on system reliability of the scraper chain, it is verified that the proposed method is applicable. And in the last section, several conclusions of this paper are summarized.

2. The reliability modeling of the scraper chain

Scraper chains as the load bearing and traction members of the scraper conveyor play an important part in accomplishing the material conveying work. As illustrated in the Fig. 2, 1 and 2 respectively refers to the plate chain and the vertical chain. According to the theory of machines and mechanisms, there are multiple failure modes in the chain transmission system such as excessive elastic elongation, tensile strength failure, etc. Considering the failure interaction, the reliability model for different failure modes of the scraper chain transmission system is, firstly, defined in order to investigate the reliability with multiple failure modes.

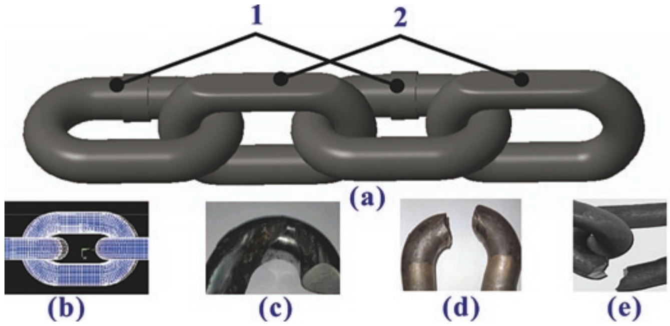

Fig. 2. 3D model and failure modes of scraper chains (a) 3D model of scraper chains, (b) Failure of elongation, (c) Failure of contact, (d) Failure at crown, (e) Failure at shoulders

2.1. Reliability model based on the elongation of scraper chains

As shown in Fig. 3, (a) represents a three-dimensional diagram of the scraper chain; (b) denotes the geometry of scraper chains and F_c is the axial tensile force; (c) indicates the force analysis of one quarter of the scraper chain. During the working process, the scraper chain is subjected to the axial pulling force. And one quarter of the scraper chain with the axial load is taken as the research object for the scraper chain structure is symmetrically distributed. In addition, two important simplifying assumptions are made to establish the reliability model based on the elongation of scraper chains.

(1) The material of scraper chains is uniform, isotropic, and conforms to the elastic characteristics;

(2) The scraper chain is subject to small deformation and conforms to the assumption of small deformation.

According to force analysis of the scraper chain, the section AB is subjected to a axial tension $N=F_c/2$ and a bending moment M_0. On any section Q of the circular arc segment BC, the bending moment $M(\alpha)$, the axial tension $N(\alpha)$ and the shearing force $Q(\alpha)$ of the scraper chain can be expressed as follows:

$$M_0=\frac{F_c r_c^2(2-\pi)}{4EJ_2}\left(\frac{l_c}{EJ_1}+\frac{\pi r_c}{2EJ_2}\right)^{-1}, \tag{1}$$

$$M(\alpha)=M_0+\frac{F_c r_c(1-\cos\alpha)}{2}, \tag{2}$$

$$N(\alpha)=\frac{F_c}{2}\cos\alpha, \tag{3}$$

$$Q(\alpha)=-\frac{F_c}{2}\sin\alpha. \tag{4}$$

Based on mechanics and geometry, the following equations can be obtained:

$$r_c = r_b + a/2, \tag{5}$$

$$l_c = L_c/2 - a/2, \tag{6}$$

$$J_1 = \pi r_b^4/4, \tag{7}$$

$$J_2 = J_1 + \Delta r_c^2 B, \tag{8}$$

$$\Delta r_c = r_c - r_b^2\left\{2r_c\left[1-\sqrt{1-\left(\frac{r_b}{r_c}\right)}\right]\right\}^{-1}, \tag{9}$$

where F_c denotes the tensile force of the scraper chain; r_b represents the size of scraper chains; a denotes the inner width of scraper chains; L_c is the pitch of scraper chains; J_1, J_2 express the section modulus of the straight-line segment and the circular arc segment, respectively.

As shown in Fig. 3 (c), the deformation energy of a quarter scraper chain is composed of two parts: the straight segment AB and the circular arc segment BC. So the total deformation energy can be expressed as follows:

$$U = U_1 + U_2 = \int_0^{l_c}\left(\frac{M_0}{2EJ_1} + \frac{N^2}{2EB}\right)dx + \int_0^{\pi/2}\left(\frac{M(\alpha)^2}{2EJ_2} + \frac{N(\alpha)^2}{2EB} + \frac{Q(\alpha)^2}{2GB}\right)r_c d\alpha, \tag{10}$$

in which E denotes the equivalent elastic modulus; μ is the Poisson ratio; G denotes the shearing elastic modulus, $G=E/(2\text{-}2\mu)$; B denotes the cross sectional area of scraper chains, $B = \pi r_b^2$.

Substitute equations (1-4) into the equation (10), then the total deformation energy can be rewritten as:

$$U = \frac{M_0 l_c}{2EJ_1} + \frac{N^2 l_c}{2EB} + \frac{r_c}{2EJ_2}\left(M_0 - Nr_c\right)\left[\frac{\pi}{2}\left(M - Nr_c\right) + 2Nr_c\right] + \frac{\pi}{4}\frac{r_c}{2EJ_2}N^2 r_c^2 + \frac{\pi}{4}\frac{N^2 r_c}{2EB} + \frac{\pi}{4}\frac{N^2 r_c}{2GB}. \tag{11}$$

According to equation (11), the displacement of the point A can be expressed as follows:

$$x_A = \Delta L_1 + \Delta L_2 + \Delta L_3, \tag{12}$$

where:

$$\Delta L_1 = \frac{M_0 l_c}{2EJ_1}\frac{\partial M}{\partial N} + \frac{Nl_c}{EB},$$

$$\Delta L_2 = \frac{\pi N r_c}{4}\left(\frac{1}{EB} + \frac{1}{GB}\right),$$

$$\Delta L_3 = \frac{\pi N r_c^3}{4EJ_2} + \frac{r_c}{2EJ_2}\left(M_0 - Nr_c\right)\left[\frac{\pi}{2}\left(k_0 - r_c\right) + 2r_c\right] + \frac{r_c}{2EJ_2}\left(k_0 - r_c\right)\left[\frac{\pi}{2}\left(M_0 - Nr_c\right) + 2Nr_c\right],$$

$$k_0 = \frac{\partial M_0}{\partial N} = \frac{\left(\frac{\pi}{2} - 1\right)\frac{r_c^2}{J_2}}{\frac{l_c}{J_1} + \frac{\pi r_c}{2J_2}}.$$

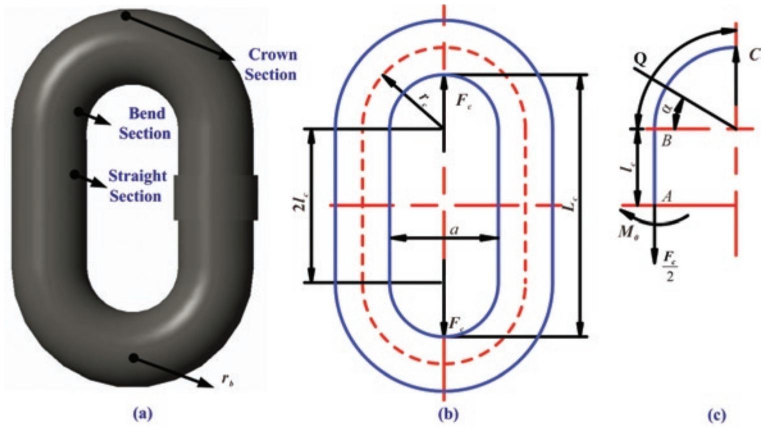

Fig. 3. 3D model, Geometry and force analysis of the scraper chain, (a) 3D model, (b) Geometry, (c) Force analysis

For a complete scraper chain, there is not only the elastic elongation $2x_A$ between scraper chains, but also the elastic compression ϖ in the contact area. The elastic compression ϖ can be defined as follows:

$$\varpi = 3F_c\sqrt[3]{\frac{r_c\left(1-\mu^2\right)^2}{12E^2 F_c r_b\left(r_c + r_b\right)}} \tag{13}$$

So the total elongation of the scraper chain can be expressed as:

$$\Delta l = \frac{\Delta L}{L_c} = \frac{2\lambda_1 x_A + \lambda_2\varpi}{L_c} = \frac{2\lambda_1\left(\Delta L_1 + \Delta L_2 + \Delta L_3\right) + \lambda_2\varpi}{L_c} \tag{14}$$

Put equations (12) and (13) into equation (14). And the total elongation of the scraper chain can be rewritten as:

$$\Delta l = \lambda_1\left\{\frac{M_0 l_c r_c^2(2-\pi)}{EJ_1\left(l_c + \pi r_c\right)} + \frac{F_c l_c}{EB} + \frac{F_c \pi r_c}{4}\left(\frac{1}{EB} + \frac{1}{GB}\right) + \frac{F_c \pi r_c^3}{4EJ_2} + \frac{r_c}{EJ_2}\left(M_0 - \frac{F_c r_c}{2}\right)\left[\left(k_0 - r_c\right)\frac{\pi}{2} + 2r_c\right] + \frac{r_c}{EJ_2}\left(k_0 - r_c\right)\left[\left(M_0 - \frac{F_c r_c}{2}\right)\frac{\pi}{2} + F_c r_c\right]\right\}L_c^{-1} + \frac{3\lambda_2 F_c}{L_c}\sqrt[3]{\frac{r_c\left(1-\mu^2\right)^2}{12E^2 F_c r_b\left(r_c + r_b\right)}}, \tag{15}$$

where λ_1, λ_1 denote the correction coefficient of the scraper chain elongation.

And so the limit state function can be defined as:

$$g_1(\boldsymbol{X}) = [\delta] - \frac{\Delta l}{L_c} \times 100\%, \tag{16}$$

in which X is the vector of the basic random variables; $[\delta]$ represents the threshold of the scraper chain elongation.

2.2. Reliability model based on the tensile strength of scraper chains

As illustrated in the Fig. 4, the force of the scraper chain is simplified to a mechanical model. For the convenience of calculation, it is assumed that each section of the scraper chain is identical and circular; the arc radius is a constant; the stress distribution of each cross section is linearly related; and the scraper chain is subject to the tensile load F_c along its axis direction. Owing to geometrical symmetry, half of the scraper chain is regarded as the research object. The surface stress of the scraper chain with pure tensile load is computed by the formula for calculating the surface stress of curved beams. According to the calculation results, the inside of its straight section and the outside of the partial circular arc withstand tensile stress, while the outside of the straight section and the partial inside circular arc withstand compressive stress, when the scraper chain bears a tensile load.

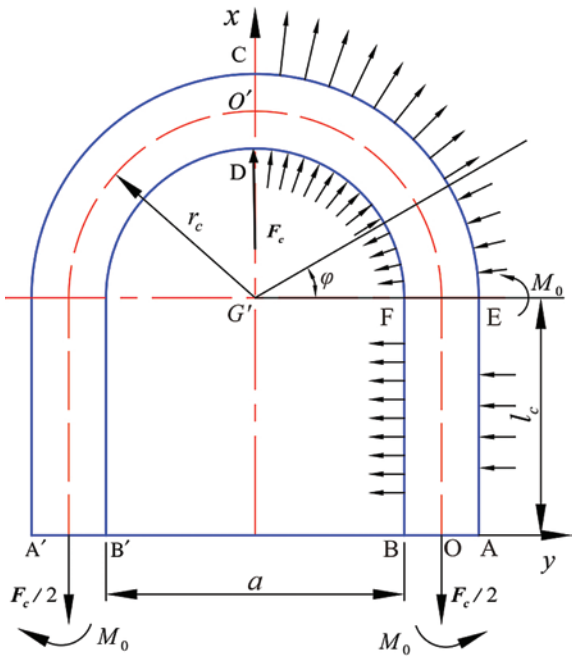

Fig. 4 Force analysis of half of the scraper chain.

Based on the force analysis of scraper chains, there are the axial tension $F_c/2$ and the bending moment M_0 on the cross-section AB, which are certain in the straight section. As shown in Fig. 4, the bending moment on any section Q of the arc section is given by:

$$M = M_0 + F_c r_c \left(1-\cos\varphi\right)/2. \tag{17}$$

When $\varphi = \pi/2$, $\cos\varphi = 0$, then the maximum bending moment of the arc segment is transformed into:

$$M_{\max} = M_0 + \frac{F_c r_c}{2}. \tag{18}$$

According to the surface stress calculation formula of curved beams, the surface stress of the circular arc segment can be defined as:

$$\sigma_y = \frac{F_x}{B} + \frac{M}{Br_c} + \frac{My}{B\mathrm{K}r_c\left(r_c + y\right)}. \tag{19}$$

When $\varphi = \pi/2$, $F_x = 0$, $M = M_{\max}$, then the stress on the outside of the section CD (Point C $y = r_b$) is transformed into:

$$\sigma_{y1} = \frac{M_{\max}}{Br_c} + \frac{M_{\max} r_b}{B\mathrm{K}r_c\left(r_c + r_b\right)} = \frac{M_{\max}}{Br_c}\left[1 + \frac{1}{\mathrm{K}\left(\varepsilon+1\right)}\right]. \tag{20}$$

Similarly the stress on the inside of the section CD (Point D $y = -r_b$) of the arc segment can be denoted as follows:

$$\sigma_{y3} = \frac{M_{\max}}{Br_c} - \frac{M_{\max} r_b}{\mathrm{K}Br_c\left(r_c - r_b\right)} = \frac{M_{\max}}{Br_c}\left(1 - \frac{1}{\mathrm{K}\left(\varepsilon-1\right)}\right), \tag{21}$$

in which K represents the neutral layer coefficient of the scraper chain cross section; and ε can be defined as follows:

$$\varepsilon = \frac{r_c}{r_b}.$$

The straight section of the scraper chain is subjected to the axial tensile load $F_c/2$ and the bending moment M_0, so the surface stress on the outside of the section AB (Point A) can be expressed as:

$$\sigma_{Z1} = \frac{F_c}{2\pi r_b^2} + \frac{M_0 r_b}{J_1}. \tag{22}$$

Similarly, the surface stress on the inside of the section AB (Point B) is shown as follows:

$$\sigma_{Z3} = \frac{F_c}{2\pi r_b^2} - \frac{M_0 r_b}{J_1}. \tag{23}$$

And so the limit state function based on the tensile strength is modeled as:

$$g_2\left(X\right) = \sigma_{Z\lim} - \sigma_{Z3}, \tag{24}$$

in which X is the vector of the basic random variables; $\sigma_{Z\lim}$ expresses the threshold of tensile strength.

2.3. Reliability model based on the contact strength of scraper chains

As shown in Fig. 5, the contact between two scraper chains is simplified as the contact between two spheres. The deformation and stress in the contact area are called contact deformation and contact stress when the two scraper chains press each other tightly. Hertz's classical theory of contact focused primarily on non-adhesive contact where no tension force is permitted to occur within the contact area [16, 18]. Therefore, assumptions are made as follows to solve the contact problem between scraper chains:

(1) Strains of scraper chains are small and within the elastic limit;
(2) The contact area of scraper chains is so small that each scraper chain can be regarded as an elastic half-space;
(3) There is a linear relation between stress and strain, and the stress depends only on the strain rather than the strain rate;

(4) The scraper chain is frictionless.

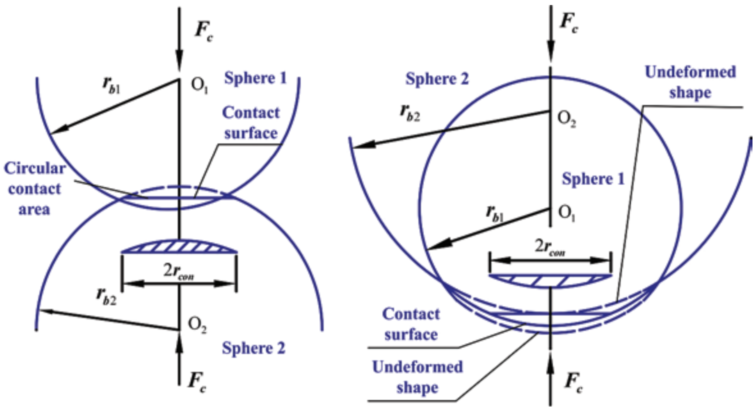

Fig. 5. External and internal contact between two spheres, (a) External contact, (b) Internal contact.

The radius of the contact area is given by:

$$r_{con} = \sqrt[3]{\frac{3F_c\left(\frac{1-\mu_1^{\ 2}}{E_1}+\frac{1-\mu_2^{\ 2}}{E_2}\right)}{4\left(\frac{1}{r_{b1}}+\frac{1}{r_{b2}}\right)}}, \tag{25}$$

where r_{b1}, r_{b2} respectively represent the radii of the two contact scraper chain bars, $r_{b1} = r_{b2} = r_b$; E_1, E_2 denote the equivalent elastic modulus, respectively, $E_1 = E_2 = E$; μ_1, μ_2 are the Poisson's ratios of the two contact scraper chains, respectively, $\mu_1 = \mu_2 = \mu$.

The maximum stress at the center of the contact area is defined as follows:

$$\sigma_{\mathrm{H}} = \frac{3F_c}{2\pi r_{con}^{\ 2}}. \tag{26}$$

Substitute equation (25) into equation (26). And the maximum contact stress σ_{H} can be rewritten as follows:

$$\sigma_{\mathrm{H}} = \frac{1}{\pi}\sqrt[3]{6F_c\left[\frac{\left(\frac{1}{r_{b1}}+\frac{1}{r_{b2}}\right)}{\left(\frac{1-\mu_1^{\ 2}}{E_1}+\frac{1-\mu_2^{\ 2}}{E_2}\right)}\right]^2}, \tag{27}$$

Similarly, the limit state function can be calculated as follows:

$$g_3(\boldsymbol{X}) = \sigma_{\mathrm{H\,lim}} - \sigma_{\mathrm{H}}, \tag{28}$$

in which $\boldsymbol{X}$ is the vector of the basic random variables; $\sigma_{H\,\mathrm{lim}}$ denotes the threshold of contact strength.

3. System reliability modeling with Copula function

3.1. Marginal probability of failure estimation by stochastic perturbation technique

The matrix description of the first four moments of the state function is obtained through the way of Taylor series expansion approximation based on the first four moments of the basic random variable vector $\boldsymbol{X}=(X_1, X_2, \ldots, X_n)^{\mathrm{T}}$. Expand the first-order approximate Taylor series of the state function and the equation below can be obtained:

$$\mathrm{g}(\boldsymbol{X}) = \mathrm{g}(\mu\mathrm{x}) + \frac{\partial \mathrm{g}_\mu}{\partial \boldsymbol{X}^{\mathrm{T}}}(\boldsymbol{X}-\mu\mathrm{x}), \tag{29}$$

in which $\frac{\partial \mathrm{g}_\mu}{\partial \boldsymbol{X}^T}$ represents the derivative of the state function to the random variable in the mean values μ.

According to the first-order approximation of Taylor series expansion, the mean of the state function is obtained as follows:

$$\mu_g = \mathrm{E}(\mathrm{g}(\boldsymbol{X})) \approx \mathrm{g}(\mu\mathrm{x}). \tag{30}$$

And the variance of the state function g($\boldsymbol{X}$) can be defined as:

$$\sigma_g^{\ 2} = \mathrm{E}\left(\left(g(\boldsymbol{X})-\mu_g\right)^2\right) = \mathrm{E}\left(\left(\frac{\partial g_\mu}{\partial X^{\mathrm{T}}}\right)(\boldsymbol{X}-\mu\mathrm{x})(\boldsymbol{X}-\mu\mathrm{x})^T\left(\frac{\partial g_\mu}{\partial \boldsymbol{X}}\right)\right), \tag{31}$$

Based on the Taylor series expansion and the first-order approximate of the state function $g(\boldsymbol{X})$, the third moment of the state function θ_g can be expressed as follows:

$$\begin{aligned}\theta_g &= \mathrm{E}\left(\left(\mathrm{g}(\boldsymbol{X})-\mu_g\right)^3\right)\\ &= \mathrm{E}\left(\left(\frac{\partial \mathrm{g}_\mu}{\partial \boldsymbol{X}^{\mathrm{T}}}(\boldsymbol{X}-\mu\mathrm{x})\right)\otimes\left((\boldsymbol{X}-\mu\mathrm{x})^T\frac{\partial \mathrm{g}_\mu}{\partial X}\right)\otimes\left((\boldsymbol{X}-\boldsymbol{\mu}\mathbf{x})^T\frac{\partial \mathrm{g}_\mu}{\partial \boldsymbol{X}}\right)\right)\end{aligned} \tag{32}$$

Similarly, the fourth moment of the state function can be expressed as follows:

$$\begin{aligned}\eta_g &= \mathrm{E}\left(\left(\mathrm{g}(\boldsymbol{X})-\mu_g\right)^4\right)\\ &= \mathrm{E}\left(\left(\frac{\partial \mathrm{g}_\mu}{\partial \boldsymbol{X}^{\mathrm{T}}}(\boldsymbol{X}-\mu\mathrm{x})\right)\otimes\left((\boldsymbol{X}-\mu\mathrm{x})^{\mathrm{T}}\frac{\partial \mathrm{g}_\mu}{\partial X}\right)\right.\\ &\quad\left.\otimes\left(\frac{\partial \mathrm{g}_\mu}{\partial X^{\mathrm{T}}}(\boldsymbol{X}-\mu\mathrm{x})\right)\otimes\left((\boldsymbol{X}-\mu\mathrm{x})^{\mathrm{T}}\frac{\partial \mathrm{g}_\mu}{\partial X}\right)\right)\end{aligned} \tag{33}$$

Based on the given limit state function, the reliability index can be defined by the first four moments:

$$\beta_F = \frac{3\mu_g\eta_g - 3\mu_g\sigma_g^{\ 4} + \theta_g\mu_g^{\ 2} - \theta_g\sigma_g^{\ 2}}{\sqrt{9\eta_g^{\ 2}\sigma_g^{\ 2} - 5\theta_g^{\ 2}\eta_g - 18\sigma_g^{\ 6}\eta_g + 5\theta_g^{\ 2}\sigma_g^{\ 4} + 9\sigma_g^{\ 10}}}, \tag{34}$$

in which $\mu_g, \sigma_g, \theta_g$ and η_g represent the mean, variance, the third moment and the forth moment of the limit state function of each failure mode.

Based on the fourth moment method, the scraper chain reliability can be defined by the reliability index β_F :

$$R_F = \Phi(\beta_F), \tag{35}$$

in which $\Phi(\bullet)$ is the standard normal distribution.

3.2. System failure probability estimation with Copulas and narrow bounds

The Copula function is actually a function that connects the joint distribution function with their respective marginal distributions, which can describe the correlation between variables commendably. The Copula function was firstly used in the financial analysis field. And it has been progressively extended to the fields of structural reliability, meteorological, hydrological, and so on in recent years [12]. As a tool of the dependence mechanism between variables, the Copula function contains almost all the dependent information of random variables. It is extremely appropriate when it is uncertain whether the correlation between variables can be calculated by the traditional linear correlation coefficient. What's more, there is a complicated correlation between the reliability of different failure modes. Based on the superiority of Copula functions in describing correlations, we proposed a system reliability model based on Copula functions and verified by the narrow-bound theory. And here, several Copula functions used in this paper are expressed as follows:

The Gaussian Copula belongs to the Elliptical Copulas, which can easily characterize the correlation between random variables without any assumptions about the marginal distribution. So it becomes one of the most widely used Copula functions. And the Gaussian Copula functions can be defined as:

$$\Phi_2\left(\Phi^{-1}(v_1), \Phi^{-1}(v_2); \alpha\right), \qquad \alpha \in [-1,1] \tag{36}$$

where α denotes the correlation coefficient; $\Phi(\bullet)$ is standard normal distribution functions; $\Phi_2(\bullet)$ represents the binary normal distribution function.

Let $\phi(\bullet) = (-\ln t)^\alpha$ be the generator, the Gumbel Copula can be expressed as follows:

$$C_G(v_1, v_2; \alpha) = \exp\left(-\left[(-\ln v_1)^{\frac{1}{\alpha}} + (-\ln v_2)^{\frac{1}{\alpha}}\right]^\alpha\right). \qquad \alpha \in (0,1] \tag{37}$$

When $\alpha = 1$, the random variable v_1, v_2 is independent, $C_G(v_1, v_2; 1) = v_1 v_2$. When $\alpha \to 0$, the random variables v_1 and v_2 are completely dependent, $\lim_{x\to 0} C_G(v_1, v_2; \alpha) = \min(v_1, v_2)$.

The Frank Copula is one of the primary copulas identified in the statistical sciences, which can describe the both of non-negative and negative correlations among variables. The expression of Frank Copula is as follows:

$$C_F(v_1, v_2; \alpha) = -\frac{1}{\alpha}\ln\left(1 + \frac{\left(e^{-\alpha v_1} - 1\right)\left(e^{-\alpha v_2} - 1\right)}{e^{-\alpha} - 1}\right) \qquad \alpha \in \mathbb{R}\setminus\{0\}. \tag{38}$$

The generator of this family is given by $\varphi(t) = -\ln\frac{e^{\alpha t} - 1}{e^{\alpha} - 1}$.

When (α=1), it indicates a positive (negative) correlation between random variables; and when $\alpha \to 0$, it means that the random variables tend to be independent of each other. What's more, the correlation parameter α of the Frank Copula function number has a one-to-one correspondence with the traditional correlation and consistency measure. The density distribution of Frank Copula is symmetrical and can be used to construct a joint distribution of random variables with symmetric correlation. In addition, since the variables are progressively independent at the end of the distribution, the Frank Copula function cannot capture the asymmetrical relationship between random variables.

As an asymmetric Archimedes copula, the negative tail of Clayton copulas shows a stronger dependence than the positive tail. With the generator $\varphi(t) = (t^\alpha - 1)/\alpha$, the Clayton Copula is given by:

$$C_C(v_1, v_2; \alpha) = \max\left(\left(v_1^{-\alpha} + v_2^{-\alpha} - 1\right)^{-\frac{1}{\alpha}}, 0\right), \qquad \alpha \in (-1,0) \cup (0,+\infty) \tag{39}$$

in which α is the relevant parameter in Clayton Copula. When $\alpha \to 0$ the random variables tend to be completely independent, $\lim_{x\to 0} C_C(v_1, v_2; \alpha) = v_1 v_2$; when $\alpha \to \infty$, the random variables tend to be completely correlated, $\lim_{x\to\infty} C_C(v_1, v_2; \alpha) = \min(v_1, v_2)$.

In addition, the probability density functions (PDFs) and contour plots of these Copulas are drawn in Appendix A, which illustrates the basic property of each Copula function. Density and contour of density of the four Copulas are shown in Appendix B. As shown in Appendix B, the density distribution of Gumbel Copulas is a "J" type distribution. In other words, the Gumbel Copula is highly sensitive to the change of the upper tail correlation between variables, but it's hard to capture the change of the lower tail distribution. Comparing the distribution diagram of the Gumbel and Clayton Copula functions, we found that both of their density functions are asymmetrical. However, contrary to the distribution of the function of Gumbel Copula, the density function of Clayton Copula is in the shape of "L". So the Clayton Copula function is highly sensitive to the change of the lower tail distribution. Actually, Clayton Copulas can quickly capture the changes related to the lower tail and can be used to describe the correlation with the characteristics of the lower tail. Since the density function of Frank Copulas is "U" shaped and has symmetry, it is impossible to capture the asymmetrical correlation between random variables. The three Archimedes Copula functions described above have different descriptions of the related structures between variables, covering various situations of related structural changes, and their excellent characteristics make them widely used in the field of reliability analysis.

The potential marginal distributions can be arbitrary and approximated with the moment-based saddle point technique [5, 6]. It is worth noting that the selected Copulas only describe the dependence characteristics of variables of the scraper chain, which are independent of the marginal distribution of failure modes. Despite some high-dimensional Copula functions are expected to be available; the undetermined parameters in high-dimension Copulas are inaccessible.

The system reliability range obtained by the traditional independent hypothesis theory is too large to meet the actual needs. Ditlevsen [4] considered the correlation between failure modes and proposed a method to calculate the reliability of second-order narrow-bound theory:

$$\begin{cases} P_f \le P_f^{\ U} = \sum_{i=1}^{n} P_{fi} - \sum_{i=2}^{n} \max P_{fij}, \\ P_f \ge P_f^{\ L} = P_1 + \sum_{i=2}^{n} \max \left(P_i - \sum_{j=1}^{i-1} P_{fij}, 0 \right), \end{cases} \quad (j < i) \tag{40}$$

4. Reliability-based optimal design with Copula function

Reliability-based optimal design is the most economical way to solve the problem of optimizations under uncertainty. The primary task of the optimization design based on reliability is to satisfy the structural reliability [8, 21]. Based on the principle above, the reliability-based optimal design of the scraper chain with multiple failure modes can be described by the following mathematical model:

$$\left.\begin{array}{l} \text{find} \quad \bar{\boldsymbol{Y}} \\ \min \quad f(\bar{\boldsymbol{Y}}) = f_{\text{sub}}(\bar{\boldsymbol{Y}}) \\ \text{s.t.} \quad R_{\text{sys}} \ge \text{R}_{\text{sys}0}, \\ \qquad \bar{\boldsymbol{Y}}^L \le \bar{\boldsymbol{Y}} \le \bar{\boldsymbol{Y}}^U, \\ \qquad q_{\text{j}}(\bar{\boldsymbol{Y}}) \ge 0, \ (\text{j}=1,\ldots,\text{m}) \end{array}\right\} \tag{41}$$

in which $f_{\text{sub}}(\bar{Y})$ is the sub-objective function; R_{sys} is system reliability; R_{sys0} is the target reliability that should be satisfied; $\bar{\boldsymbol{Y}}^{\boldsymbol{L}}, \bar{\boldsymbol{Y}}^{U}$ are the upper and lower bounds of the design variable $\bar{\boldsymbol{Y}}$; $q_j(\bar{\boldsymbol{Y}})$ is the inequality constraint.

What's more, the flow chart of system reliability-based optimal design processes for the scraper chain is depicted in Fig. 6, which pursuits the most economical and rational structure.

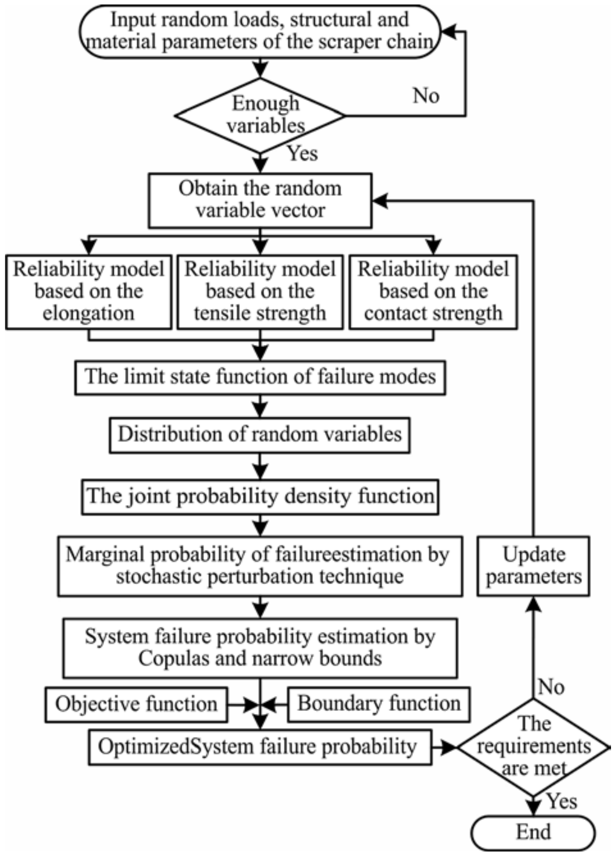

Fig. 6. The flow chart of the optimization process based on system reliability

5. Illustrative example

In this section, the φ14×50 scraper chain, produced of 23MnNiCrMo, is used as an illustrative example to verify the rationality of the proposed method. According to the standard of *high-tensile steel chains (round link) for chain conveyors and coal ploughs* (*ISO 610:1990*), the random variables of the scraper chain are therefore defined, including the geometrical dimensions, material properties and the tensile force applied to the scraper chain. The probability properties of defined variables are summarized in Table 1. Meanwhile, the distributions of random variables are shown in the Fig. 7.

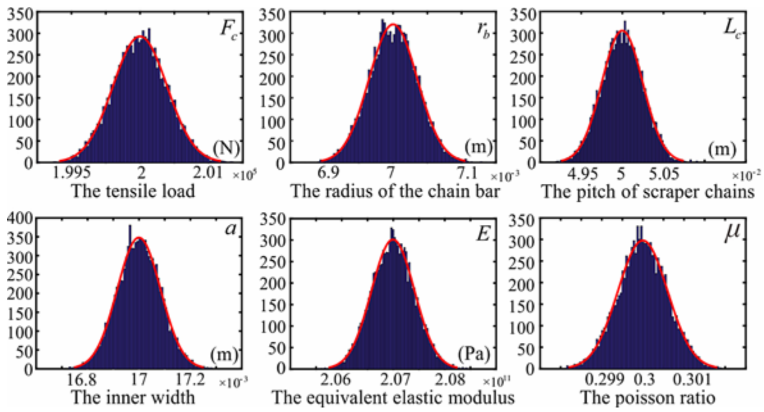

Fig. 7. Normally distribution of random variables

Table 1. The distribution details of design variables in this study

Variables	Mean	Standard deviation	Distribution	Unit
F_c	2×10^{5}	0.002	Normal	N
r_b	7×10^{-3}	0.005	Normal	m
L_c	5×10^{-2}	0.005	Normal	m
a	1.7×10^{-2}	0.005	Normal	m
E	2.07×10^{11}	0.002	Normal	Pa
μ	0.3	0.002	Normal	-

Note:The symbol "-" denotes the dimensionless variables without units.

5.1. System failure probability estimation with selected Copulas

In this section, three different reliability models of scraper chains were separately analyzed in order to obtain the failure probability. The reliability model is constructed by the reliability index approach (RIA), in which the reliability index interval is employed to evaluate the reliability degree of an uncertain structure. The reliability index, the reliability, and the failure probability related to the known probability information of each failure modes are shown in Table 2. And it becomes apparent that contact failure is one of the most likely failure modes for the probability of the contact failure is up to 9.954×10^{-2} with the test forces F_c; in addition, the probable failure due to the excessive elastic elongation is 1.063×10^{-2}; by the way, it is gratifying

Table 2. The reliability index, the reliability, and the failure probability of single failure modes

Reliability Index	Reliability	Failure Probability
β_1=2.3034	R_1=0.98937	P_{f1}=0.01063
β_2=3.8370	R_2=0.99994	P_{f2}=0.00006
β_3=1.2842	R_3=0.90046	P_{f3}=0.09954

that tensile strength failure of the scraper chain is almost impossible because its failure probability is only 6.23×10^{-5}.

The Kendall rank correlation is a non-parametric test that measures the strength of dependence between two variables. And its correlation coefficient ranges from -1 to 1. When τ is 1 (-1), it means that two random variables have a positive (negative) correlation; when τ is 0, it means that the two random variables are independent of each other. In order to indicate the strength of dependence between two variables, the Kendall rank correlation coefficients of any two failure modes are listed as follows:

$$\begin{aligned} K_{rcc12} &= 0.5964 \\ K_{rcc13} &= 0.2427 \\ K_{rcc23} &= 0.5547 \end{aligned} \tag{42}$$

Based on the analysis of various Copula functions, it is found that Gaussian Copula has the lowest AIC value and the best fitting effect. Gaussian Copula is the most widely used Copula function, which can easily characterize the correlation between random variables without any assumptions about the marginal distribution. And the parameters and AIC values for the Gaussian, Gumbel, Frank, and Clayton Copula functions are shown in Table 3:

Table 3. The parameters and AIC values of different Copula functions

	Gaussian [α, AIC]	Gumbel [α, AIC]	Frank [α, AIC]	Clayton [α, AIC]
g_1g_2	0.806, **-1.047×10^4**	2.477, -9.510×10^3	7.833, -9.507×10^3	2.955, -6.247×10^3
g_1g_3	0.372, **-1.492×10^3**	1.321, -1.219×10^3	2.296, -1.354×10^3	0.641, -9.282×10^2
g_2g_3	0.765, **-8.811×10^3**	2.246, -7.870×10^3	6.831, -8.004×10^3	2.491, -5.254×10^3

Note: the AIC values are bold and underline if the corresponding Copula is preferred.

Aiming at the joint failure probability modelling problems, a method for estimating the failure probability of scraper chains based on system reliability is proposed. The Copula function is used to describe the dependent structure of the two failure modes, and the AIC method is used to determine the optimal fitting correlation function. The system reliability is calculated by the stochastic perturbation technique and the four-moment method of the reliability system. And the scatter plots of the different failure modes of the scraper chain are shown in Fig. 8:

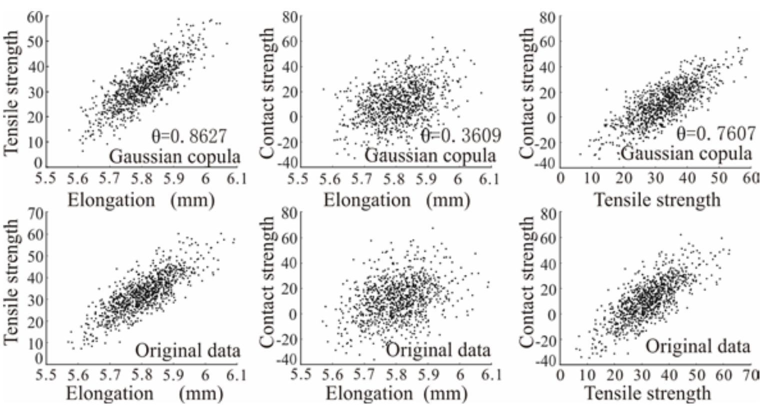

Fig. 8. The scatter plots of multiple failure modes

Considering three correlated failure modes, the failure probability and the reliability of the scraper chain are defined by the Copula theory:

$$\begin{aligned} P_{fsys} &= 0.1064, \\ R_{sys} &= 1\text{-}P_{sys} = 0.8936. \end{aligned} \tag{43}$$

5.2. System reliability-based design optimization of scraper chains

The mass of the scraper chain is a significant parameter of the scraper chain. The redundancy mass not only reduces the efficiency of the scraper conveyor but also aggravates the wear of the middle trough. Therefore, it is necessary to make the reliability-based optimal design model of the scraper chain throughout the design process to minimize the mass of scraper chains. Based on the optimal design principle involving reliability, the reliability-based optimal design model of the scraper chain with multiple failure modes can be defined as follows:

$$\begin{aligned} &\text{min. mass } f(\boldsymbol{X}) = \rho\left(\left(a+2r_b\right)\pi^2 + 2\pi\left(L_c-a\right)\right)r_b^2 \\ &\text{s.t. } R_{sys} \ge \mathrm{R}_{\mathrm{sys0}} \\ &\quad a \le L_c, 2r_b \le a, \\ &\quad \boldsymbol{X}^{\mathrm{L}} \le \boldsymbol{X} \le \boldsymbol{X}^{\mathrm{U}}, \quad r_b \in \mathbb{R}^{ndv} \end{aligned} \tag{44}$$

where $\boldsymbol{X}^{\mathrm{L}}, \boldsymbol{X}^{\mathrm{U}}$ represent the lower and upper boundaries of the scraper chain design variable, respectively, $\boldsymbol{X}^{\mathrm{L}}$=[$2.0\times10^5$, 6.5×10^{-3}, 4.9×10^{-2}, 1.6×10^{-2}, 2.07×10^{11}, 0.3] and $\boldsymbol{X}^{\mathrm{U}}$=[$2.0\times10^5$, 8×10^{-3}, 5.2×10^{-2}, 1.8×10^{-2}, 2.07×10^{11}, 0.3]; ρ represents the density of the scraper chain material; And $\mathrm{R}_{\mathrm{sys0}}$ is the target system reliability probability of the scraper chain; R_{sys} represents the optimized system reliability probability.

Table 4. Comparison between initial design and optimal solution based on reliability

	Design variables ($\boldsymbol{X_i}$, **i =1,2,...,6**)	$f(\boldsymbol{X})$ (kg)	R_{sys}
Initial	(2×10^5, 7×10^{-3}, 5×10^{-2}, 1.7×10^{-2}, 2.07×10^{11}, 0.3)	0.1987	0.8936
RBDO	(2×10^5, 7.02×10^{-3}, 5.032×10^{-2}, 1.789×10^{-2}, 2.07×10^{11}, 0.3)	0.2023	0.9810

Comparison between initial design and reliability based optimal solution for the scraper chain are shown in Table 4. The result shows that in order to make the reliability of the scraper chain R_{sys} meet the requirements ($R_{sys} \ge \mathrm{R}_{\mathrm{sys0}} = 0.98$), the required minimum mass of the scraper chain has increased to 0.2023 kg. Simultaneously, the values of optimized design variables are acceptable.

6. Conclusions

Correlation problems in mechanical system reliability are ubiquitous and unavoidable. The Copula-based system reliability model provides a scientific and practical solution to the problem of system reliability modeling and system reliability based optimization. In this work, the mechanical model of each failure mode is established. And the correlation between failure modes is introduced by the Copula function theory. Then, the system reliability model of multiple failure modes is established based on the joint distribution function of Copulas. Furthermore, a system reliability-based design optimization of scraper chains with multiple dependent failure modes has been proposed. The main conclusions of this paper are as follows:

(1) The contact failure mode has the highest probability of failure. Therefore, the most effective way to increase the system reliability of the scraper chain is to reduce the failure probability of contact failure.

(2) The dependency structure between each failure mode can be described by different Copula functions, but result in different joint failure probabilities. And as shown in the illustration herein, the results obtained from the Gaussian Copula function are similar to the simulation results.

(3) A design optimization based on system reliability is performed and the corresponding optimal variables are obtained. The optimal results showed that the optimization design of the scraper chain can be achieved while meeting the requirements of target system reliability.

Acknowledgements

This work was supported by the Key Project of National Natural Science Foundation of China (Grant No. U1510205), Program for Changjiang Scholars and Innovative Research Team in University (Grant No. IRT_16R68), a project funded by the Priority Academic Program Development of Jiangsu Higher Education Institutions (PAPD).

Appendix A

Table 5. Summary of the bivariate Copula function discussed in this study

Copula	Copula function, $C(v_1,v_2;\alpha)$	Range of α
Gaussian	$\Phi_2\left(\Phi^{-1}(v_1),\Phi^{-1}(v_2);\alpha\right)$	$[-1,1]$
Gumbel	$C_G(v_1,v_2;\alpha)=\exp\left(-\left[(-\ln v_1)^{\frac{1}{\alpha}}+(-\ln v_2)^{\frac{1}{\alpha}}\right]^{\alpha}\right)$	$(0,1]$
Frank	$C_F(v_1,v_2;\alpha)=-\frac{1}{\alpha}\ln\left(1+\frac{\left(e^{-\alpha v_1}-1\right)\left(e^{-\alpha v_2}-1\right)}{e^{-\alpha}-1}\right)$	$\mathbb{R}\setminus\{0\}$
Clayton	$C_{Cl}(v_1,v_2;\alpha)=\left(v_1^{-\alpha}+v_2^{-\alpha}-1\right)^{-\frac{1}{\alpha}}$	$[-1,+\infty)\setminus\{0\}$

* v_1, v_2 *are the random variables of marginal distribution, α is the Copula parameter*

Appendix B

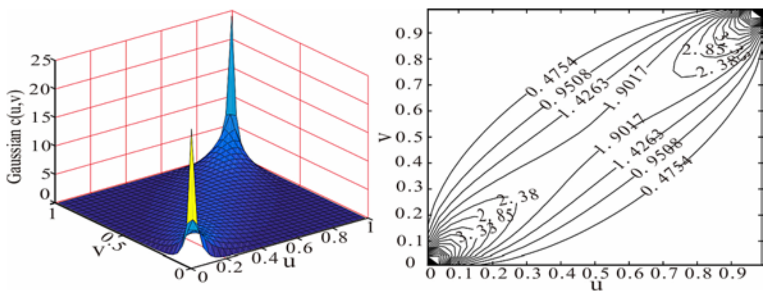

Fig. 9. The PDF and contour plot of Gaussian Copula with α=0.8627

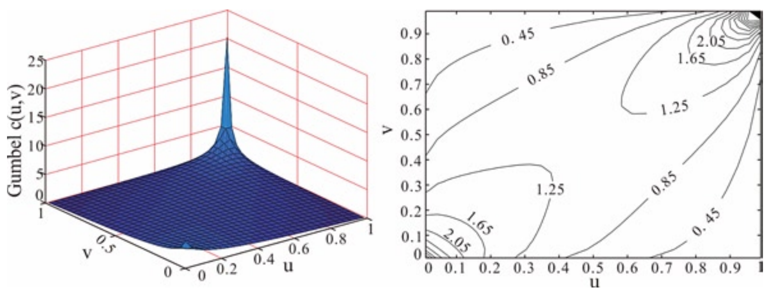

Fig. 10. The PDF and contour plot of Gumbel Copula with α=1.5

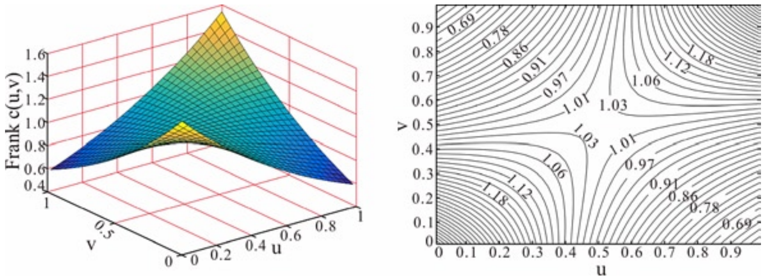

Fig. 11. The PDF and contour plot of Frank Copula with α=1

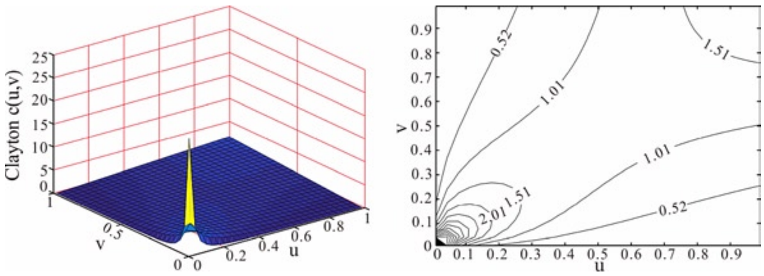

Fig. 12. The PDF and contour plot of Clayton Copula with α=1

References

1. Akaike H. Factor analysis and AIC. Psychometrika 1987; 52(3): 317-332, https://doi.org/10.1007/BF02294359.
2. Ba-abbad M A, Nikolaidis E, Kapania R K. New Approach for System Reliability-Based Design Optimization. AIAA Journal 2006; 44(5): 1087-1096, https://doi.org/10.2514/1.17237.
3. Burnham K P, Anderson D R. Model Selection and Multimodel Inference: A Practical Information-Theoretic Approach. Springer-Verlag New York 2002.
4. Ditlevsen O. Narrow Reliability Bounds for Structural Systems. Journal of Structural Mechanics 1979; 7(4): 453-472, https://doi.org/10.1080/03601217908905329.
5. Huang X, Jin S, He X, et al. Reliability analysis of coherent systems subject to internal failures and external shocks. Reliability Engineering and System Safety 2019; 181: 75-83, https://doi.org/10.1016/j.ress.2018.09.003.
6. Huang X, Li Y, Zhang Y, et al. A new direct second-order reliability analysis method. Applied Mathematical Modelling 2018; 55: 68-80, https://doi.org/10.1016/j.apm.2017.10.026.
7. Jiang C, Li W X, Han X, et al. Structural reliability analysis based on random distributions with interval parameters. Computers and Structures 2011; 89(23): 2292-2302, https://doi.org/10.1016/j.compstruc.2011.08.006.
8. Jiang C, Zhang W, Wang B, et al. Structural reliability analysis using a copula-function-based evidence theory model. Computers and Structures 2014; 143: 19-31, https://doi.org/10.1016/j.compstruc.2014.07.007.
9. Jiang S B, Zeng Q L, Wang G, et al. Contact Analysis of Chain Drive in Scraper Conveyor Based on Dynamic Meshing Properties. International Journal of Simulation Modelling 2018; 17(1): 81-91, https://doi.org/10.2507/IJSIMM17(1)418.
10. Keshtegar B. A Modified Mean Value of Performance Measure Approach for Reliability-Based Design Optimization. Arabian Journal for Science and Engineering 2017; 42(3): 1093-1101, https://doi.org/10.1007/s13369-016-2322-0.
11. Li D, Tang X, Zhou C, et al. Uncertainty analysis of correlated non-normal geotechnical parameters using Gaussian copula. Science China-Technological Sciences 2012; 55(11): 3081-3089, https://doi.org/10.1007/s11431-012-4937-z.
12. Liu P, Li L, Guo S, Xiong L, et al. Optimal design of seasonal flood limited water levels and its application for the Three Gorges Reservoir. Journal of Hydrology 2015; 527: 1045-1053, https://doi.org/10.1016/j.jhydrol.2015.05.055.
13. Lu H, Peng Y, Cao S, et al. Parameter Sensitivity Analysis and Probabilistic Optimal Design for the Main-Shaft Device of a Mine Hoist. Arabian Journal for Science and Engineering 2018; 1-9.
14. Lu H, Zhang Y. Reliability-Based Robust Design for Structural System with Multiple Failure Modes. Mechanics Based Design of Structures and Machines 2011; 39(4): 420-440, https://doi.org/10.1080/15397734.2011.560541.
15. Mishra, S K, Roy B K, Chakraborty S. Reliability-based-design-optimization of base isolated buildings considering stochastic system parameters subjected to random earthquakes. International Journal of Mechanical Sciences 2013; 75(4): 123-133, https://doi.org/10.1016/j.ijmecsci.2013.06.012.
16. Muthukumar S, DesRoches R. A Hertz contact model with non-linear damping for pounding simulation. Earthquake Engineering & Structural Dynamics 2006; 35(7): 811-828, https://doi.org/10.1002/eqe.557.
17. Nelsen R B. An Introduction to Copulas. Springer Science & Business Media 2007.
18. Patrício, P., The Hertz contact in chain elastic collisions. American Journal of Physics 2004; 72(12): 1488-1491, https://doi.org/10.1119/1.1778394.
19. Pitt, M, Chan D, Kohn R. Efficient Bayesian Inference for Gaussian Copula Regression Models. Biometrika 2006; 93(3): 537-554, https://doi.org/10.1093/biomet/93.3.537.
20. Rausand, M. System Reliability Theory: Models, Statistical Methods, and Applications. 2nd Edition. A JOHN WILEY & SONS, INC, 2004.

21. Royset J O, Der Kiureghian A, Polak E. Reliability-based optimal structural design by the decoupling approach. Reliability Engineering and System Safety 2001; 73(3): 213-221, https://doi.org/10.1016/S0951-8320(01)00048-5.
22. Sklar A. Random Variables, Distribution Functions, and Copulas: A Personal Look Backward and Forward. Lecture Notes-Monograph Series 1996; 28: 1-14, https://doi.org/10.1214/lnms/1215452606.
23. Tang X S, Li D Q, Zhou C B, et al. Copula-based approaches for evaluating slope reliability under incomplete probability information. Structural Safety 2015; 52: 90-99, https://doi.org/10.1016/j.strusafe.2014.09.007.
24. Wang H, Zhang Q. Xie F. Dynamic tension test and intelligent coordinated control system of a heavy scraper conveyor. IET Science, Measurement & Technology 2017; 11(7): 871-877, https://doi.org/10.1049/iet-smt.2016.0425.

Li SHUAI
Zhu ZHENCAI
Lu HAO
Shen GANG
School of Mechanical and Electrical Engineering
China University of Mining and Technology
No 1, Daxue Road
Xuzhou, Jiangsu, 221116
P.R. China

Jiangsu Key Laboratory of Mine Mechanical and Electrical Equipment
China University of Mining & Technology
No 1, Daxue Road
Xuzhou, Jiangsu, 221116
P.R. China

E-mails: shuaili@cumt.edu.cn; zhuzhencai@cumt.edu.cn
haolu@cumt.edu.cn; shengang@cumt.edu.cn